REGIONAL RESURFACING, SECONDARY CRATER POPULATIONS, AND CRATER SATURATION EQUILIBRIUM ON THE MOON.

R. Z. Povilaitis[1], M. S. Robinson[1], C. H. van der Bogert[2], H. Hiesinger[2], H. Meyer[1], L. R. Ostrach[3]. [1]School of Earth and Space Exploration, Arizona State University, Tempe, AZ 85287 USA (rpovilaitis@ser.asu.edu); [2]Institut für Planetologie, Westfälische Wilhelms-Universität, Münster, Germany; [3]USGS Astrogeology Science Center, Flagstaff, AZ 86001, USA.

Introduction: Impact crater density has long been used as an indicator of the relative age of surface units on the Moon. Crater density also provides direct evidence of resurfacing events. Basin-forming impacts played a large role in regional resurfacing on the Moon, as well as contributing to the current preserved crater population. The oldest areas of the Moon likely contain crater populations at or approaching saturation equilibrium - wherein the formation of a new impact crater erases a similarly sized existing crater [**1,2,3**]. Identifying the occurrence of saturation equilibrium (SEQ) is important for understanding the nature of the crater population and the effect of resurfacing and/or secondary bombardment.

The global population of lunar craters >20 km in diameter was analyzed to correlate crater distribution with resurfacing events and multiple impactor populations [**4**, Fig. 1a]. The work presented here extends the global crater distribution analysis to smaller craters (5-20 km diameters, n=22,746) [**5**]. Smaller craters form at a higher rate than larger craters and thus add granularity to age estimates of larger units and reveal smaller and younger areas of resurfacing (see also [**6**]). The resulting maps show local deficiencies of 5-20 km diameter craters, which we interpret to be caused by a combination of resurfacing by the Orientale basin, infilling of intercrater plains within the nearside highlands, and partial mare flooding of the Australe basin. Chains of 9-16 km diameter secondaries NW of Orientale and possible 5-10 km diameter basin secondaries within the farside highlands are also distinguishable. Locations where relative crater densities exceed levels thought to represent SEQ can be mapped, which allows analysis of the most heavily cratered regions of the lunar highlands (Fig. 3).

Crater Counts: All craters between 5 km and 20 km in diameter were digitized at a scale between 1:250,000 and 1:500,000 in ArcGIS. Basemaps used included: 1) a 100 m/pixel scale WAC monochrome (643 nm) mosaic with an average solar incidence of 60°, and 2) a shaded relief map based on 100 m/pixel LROC WAC Digital Elevation Model (GLD100 [**7**]) to help demarcate craters in shadowed regions at the poles and/or subdued craters. An existing database of >20 km craters supplemented this dataset [**8**].

Crater Density: We determined areal crater density for each diameter range (5-20 km and >20 km) independently using a moving neighborhood method with a radius of 500 km and an output cell size of 15 km (Fig. 1). Density magnitude values for each map were divided into 10 equal-interval bins and reclassified with a ranking of 1 to 10 (1 being lowest density and 10 being highest). The resulting 5-20 km density map (Fig. 1b) was subtracted from the >20 km density map (Fig. 1a) to produce a crater density difference map (Fig. 2). Output cell values range from -4 to +5. Positive difference values represent a high density (red) of >20 km craters relative to 5-20 km craters, and negative values represent low density (blue) of >20 km craters relative to 5-20 km craters.

Saturation Equilibrium: Seventeen crater size bins were populated with all craters within a 500 km radius of the center of each 15x15 km output cell. Relative density (R) values were calculated for each bin using the method outlined in [**9**]. Global crater density maps (Fig. 3) were then created showing those areas having R≥0.3 for each crater bin. This measure restricts the condition for SEQ to ~10% of geometric saturation.

Results: The difference map highlights several notable features with one of the most prominent being a large zero difference area encompassing the mare and several large impact basins on the nearside (area A in Fig. 2). Observing such similar behavior between mare and some highlands is consistent with a production

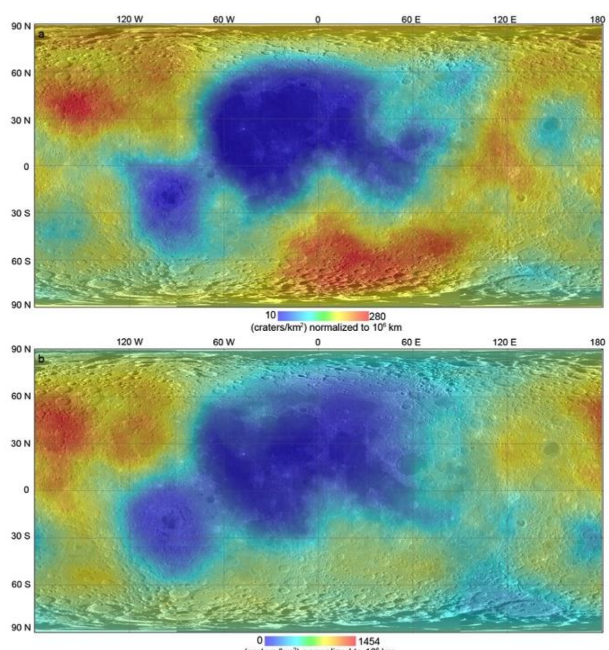

Figure 1. *Areal crater density for >20 km (a) and 5-20 km craters (b).*

function that is constant in time, rather than temporally changing proportions of different impactor types [**10**]. A positive difference area surrounding the Orientale basin (B in Fig. 2) indicates that this area has retained a greater number of >20 km craters relative to 5-20 km craters, which is expected for a basin that disrupted the existing crater population and whose continuous ejecta obliterated smaller craters out to 2 basin diameters from the rim [**4**]. To the northwest of Orientale basin, beyond this proximal affected zone, is a negative difference area peppered with chains of 5-20 km secondaries traceable back to the Orientale basin (C in Fig. 2) [**11**]. The most extreme relative differences are a widespread positive density difference in the southern nearside highlands (D in Fig. 2) and a negative density difference throughout much of the farside highlands (E in Fig. 2). An area in the heavily-cratered "pristine" NW farside highlands displays zero density difference (F in Fig. 2). Detailed analyses of CSFDs extracted from these areas are reported by **[6**].)

Figure 3 shows the areas where R≥0.3 for craters in three diameter ranges across the Moon - expanding on previous work which suggested SEQ may exist in parts of these areas [**1,12,13**]. Areal coverage for these bins is as follows: 27% (57-80 km), 39% (80-113 km), 12.4% (113-160 km). R≥0.3 for craters down to 5 km craters has also been mapped, though areal coverage of these bins is much lower (< 1% for 5-7 km craters), because these smaller craters likely reach SEQ at lower percentages of geometric saturation. Nevertheless, maps of R≥0.3 offer a way to identify the most heavily cratered areas of the Moon for focused studies.

Conclusions: 1) A significant reduction of craters >5 km in the nearside maria was caused by large-scale basaltic flooding. 2) A reduction of 5-20 km diameter craters occurred due to removal by the formation of the Orientale basin and infilling by mare basalts. 3) Tightly-grouped 9-16 km secondaries are present NW of Orientale. 4) There is a high density of >20 km craters relative to 5-20 km craters in the area encompassing the nearside highlands and Mare Australe. 5) Possible previously unrecognized 8-22 km secondaries are associated with several farside basins. 6) Large regions of the Moon contain crater densities exceeding R≥0.3, 7) Saturation equilibrium is likely a size-dependent process, where smaller craters are more quickly and efficiently destroyed than larger craters. 8) A sequence of major impact events at ~4.03, 4.15, 4.19, and 4.26 Ga suggests that major basin-forming events were not clustered around 3.9 Ga [e.g., **6,14**] arguing against a late heavy bombardment [**15,16,17,18**]. 9) The most ancient surfaces on the Moon give ages that are consistent with major resurfacing due to the formation of the South Pole-Aitken basin [see **also 6**].

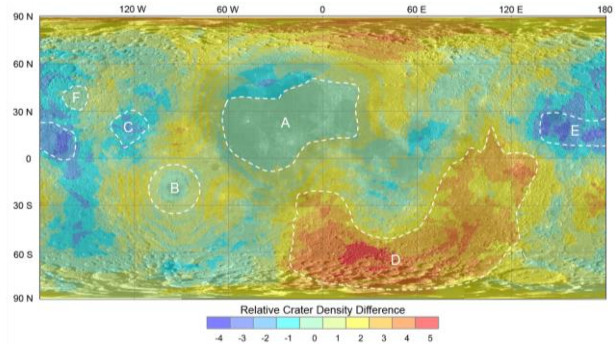

Figure 2. *5-20 km vs >20 km crater density difference.*

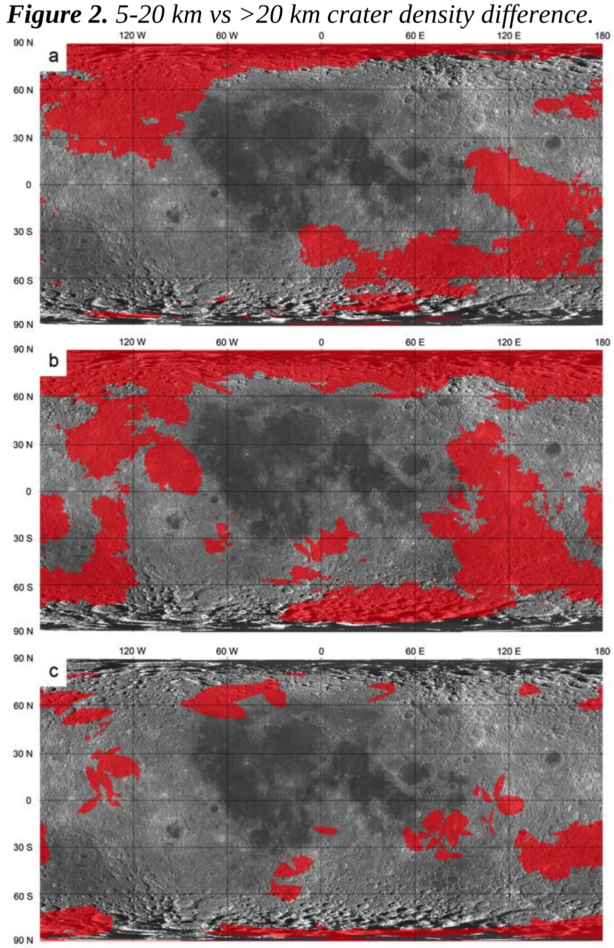

Figure 3. *Crater saturation equilibrium for (a) 57-80 km, (b) 80-113 km, and (c) 113-160 km craters.*

References: [**1**] Hartmann (1984) *Icarus* 60, 56-74. [**2**] Trask (1966) *JPL Tech. Rep. 32-800*, 252-263. [**3**] Gault (1970) *Radio Science* 5, 273-291. [**4**] Head et al. (2010) *Science* 329, 1504-1507. [5] Povilatis et al (2017) *Planet Space Sci*., in revision. [**6**] van der Bogert et al, *LPSC* 48 #1437. [**7**] Scholten et al. (2012) *JGR* 117, E00H17. [**8**] Kadish et al. (2011) LPSC 42, #1006. [**9**] Arvidson et al. (1979) *Icarus* 37, 467–474. [**10**] Wilhelms (1976) *PLPSC* 7, 2883-2901. [**11**] Neukum et al. (2001) *Space Sci. Rev*. 96, 55-86. [**12**] Richardson (2009) *Icarus* 204, 697-715. [**13**] Fassett (2011) *GRL* 38, L10202. [**14**] Xiao and Werner (2015) *JGR* 122, 2277-2292 [**15**] Hiesinger et al. (2012) *LPSC* 43, #2863. [**16**] Tera et al. (1974) *EPSL* 22, 1-21. [**17**] Wetherill (1975) *PLPSC* 6, 1539-1561 [**18**] Spudis et al. (2011) *JGR* 116, E00H03.